Simulation of F^- and HF Transport in the RPC Gas Flow

Authors: Isis Mota, L.Neubarth, D.Chalhub, R.Lucena, N.Mangiavacchi, E.Melo, A.Santoro, M.Thiel

Universidade do Estado do Rio de Janeiro – PPG-EM

The study of the transport and flushing of contaminants such as hydrofluoric acid (HF) in Resistive Plate Chambers (RPCs) [1] is essential to ensure electrode durability and muon detection efficiency. Several experimental studies have already investigated the relationship between HF concentration in RPCs and the gas flow rate. For instance, results obtained at the CERN Gamma Irradiation Facility (GIF++) showed that the HF production rate depends on both the background radiation rate and the gas flow rate, and that HF can accumulate inside the chamber if the flow rate is insufficient to remove it. These findings underscore the importance of understanding and optimizing the flow dynamics and contaminant transport in these detectors [2]. In this work, a two-dimensional numerical methodology based on the Finite Element Method (FEM) is presented to model the hydrodynamic flow and the advective-diffusive transport of hydrofluoric acid (HF) in a 2D geometric domain with an array of circular obstacles. It should be emphasized that this study focuses exclusively on the flow behavior and the flushing dynamics of HF through the chamber, without considering the adsorption or attachment of acid molecules onto the electrode surfaces.

Geometry and Mesh (Gmsh)

The 2D domain geometry was parametrized and generated using the `Gmsh` scripting language with the *kernel* `OpenCASCADE`. Boolean operations were applied to insert the internal disks into the flow channel. An adaptive local refinement was set up in regions exhibiting high velocity gradients, such as the inlet slot, outlet slot, and surrounding the disk walls, as illustrated in Figure 1. To ensure robust implementation of the boundary conditions via code, physical boundaries (*Physical Tags*) were identified purely geometrically following the boolean operation. The resulting mesh was exported in MSH2 ASCII format with unstructured triangular elements.

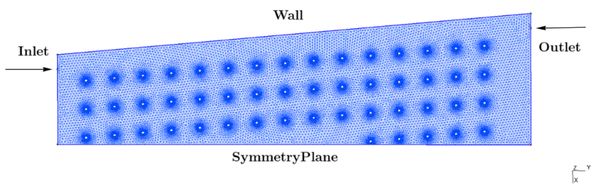


Figure 1: Unstructured bi-dimensional mesh generated in Gmsh for the channel domain, highlighting local refinement at the inlet, outlet, and around the circular obstacles.

Navier-Stokes

The steady-state incompressible flow is governed by the Navier-Stokes equations. The problem was solved in the `Julia` programming language using the `Gridap.jl` ecosystem for the Finite Element Method. The mixed element pair P_2/P_1 was employed (quadratic elements for the velocity field $\mathbf{u}$ and linear elements for the pressure field p). Numerical stabilization against oscillations was guaranteed using SUPG/PSPG formulations [3]. The applied boundary conditions include a parabolic velocity profile at the inlet $u_y = U_{\text{inlet}} \cdot 4s(1-s)$, a no-slip condition ($\mathbf{u} = \mathbf{0}$) on the walls and disks, and symmetry and free-exhaustion conditions at the *outlet*. To represent realistic operational gas renewal conditions in RPC chambers, four flow regimes based on nominal volume exchange rates per hour (0.5, 1.0, 2.0, and 3.0 Vol/h) were simulated. The characteristic velocity u_0 for each regime was obtained by dividing the corresponding volumetric flow rate by the cross-sectional area of the chamber inlet. From u_0, the density ($\rho = 4.25$ kg/m^3), and the dynamic viscosity ($\mu = 0.2$ mPa $\cdot$ s) of the dominant carrier gas (R134a, 95.2%), and adopting the chamber gap ($L_0 = 2$ mm) as the characteristic length, the simulated Reynolds numbers were determined ($Re = 1.90; 3.80; 7.61; 11.41$), as detailed in Table 1. The solution of the nonlinear system was performed using the Newton-Raphson algorithm with line search (*Backtracking*), yielding the velocity profile and streamlines presented in Figure 2.

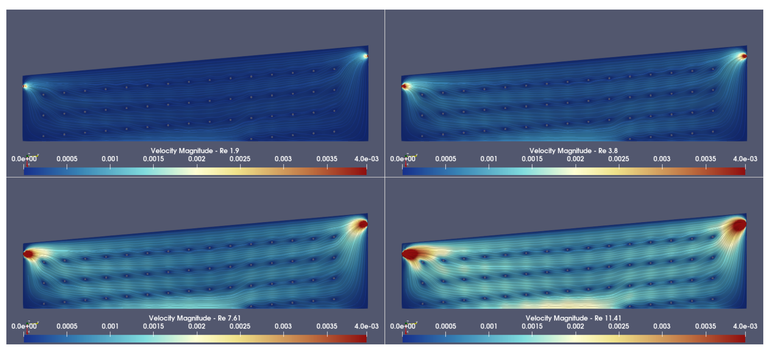


Figure 2: Distribution of velocity magnitude and streamline pattern in the channel domain for different Reynolds Numbers ($Re = 1.90$, 3.80, 7.61, and 11.41). The evolution of the laminar flow velocity profile is observed, with acceleration in restricted regions and the formation of flow patterns along the obstacle array.

Simulation	Volumetric Flow [Vol/h]	Characteristic Velocity u_0 [m/s]	Reynolds (Re)
1	0.5	0.0448	1.90
2	1.0	0.0895	3.80
3	2.0	0.1790	7.61
4	3.0	0.2690	11.41

Table 1: Operational parameters and Reynolds numbers.

Advective-Diffusive Transport

The time evolution of HF concentration (c) was modeled by the non-dimensionalized advection-diffusion equation:

$$\frac{\partial c}{\partial t} + \nabla \cdot \left(\mathbf{u}c - \frac{1}{Pe_{\text{HF}}} \nabla c \right) = 0$$

The velocity field $\mathbf{u}$ computed in the hydrodynamic stage was linearly interpolated over the P1 finite element mesh using a `Python`-based solver. The initial condition assumes a uniform concentration $c(x, y, 0) = 1.0$ throughout the fluid domain. The boundaries of the disks and walls have zero mass flux, the *inlet* acts as a watertight barrier, and the *outlet* remains the sole exhaustion boundary for HF. The cases were evaluated for the corresponding Péclet numbers ($Pe_{\text{HF}} = 14.46; 28.89; 57.79; 86.84$). The spatial evolution of the concentration field for the $Re = 11.41$ case is displayed in Figure 3. Additionally, electrophoretic transport simulations of fluorine ions (F^-) demonstrate rapid electromigration toward the electrode walls driven by the electric field [4]. In realistic RPC operation, these surface-bound ions quickly react with hydrogen donors (e.g., water vapor or isobutane) to form neutral HF, which then disperses without electric drift [5].

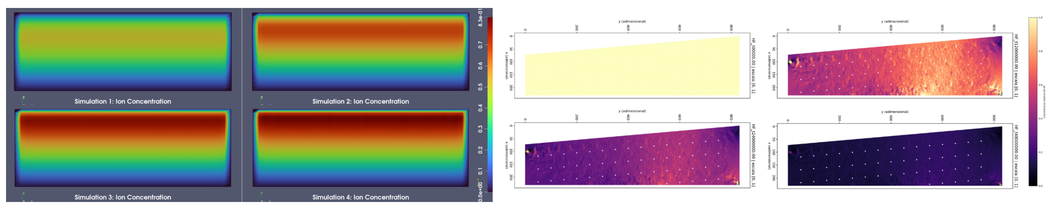


Figure 3: (a) F^- ion distribution under intense electric field drift ($E^* = 1$), showing strong accumulation near the top electrode [4]. (b) Neutral HF concentration field governed solely by advective-diffusive transport.

Results

The velocity fields obtained in `Gridap` demonstrate the formation of the parabolic profile and the recirculation regions generated by the presence of the disks. The transient simulation of transport in `Python` enabled monitoring the clearance curve of the remaining HF fraction in the domain as a function of non-dimensional time, as illustrated in Figure 4. It was observed that an increase in the Reynolds number intensifies the advective regime, significantly accelerating the rate of flushing and removal of HF gas through the exhaust boundary.

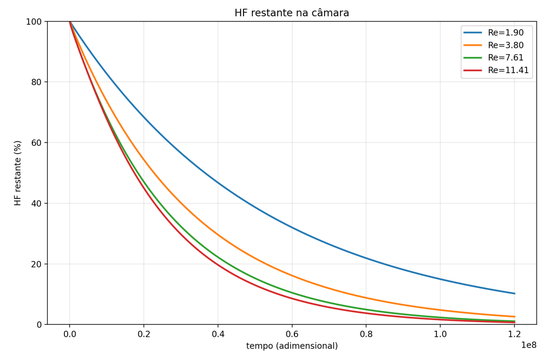


Figure 4: Time evolution of the percentage of hydrofluoric acid (HF) remaining inside the chamber for different Reynolds Numbers ($Re = 1.90$, 3.80, 7.61, and 11.41). Acceleration of the HF removal/flushing rate from the domain is observed as the convective regime is intensified with increasing Re.

Conclusions

The integration between the mesh generator `Gmsh`, the hydrodynamic solver in `Julia` (`Gridap`), and the transport tool in `Python` proved to be efficient, stable, and reproducible. The correction and refinement of the 2D mesh allowed predicting the flow dynamics and the residence time of contaminants in the RPC chambers, providing the necessary basis for assessing the detector's efficiency and degradation. Furthermore, although the simplified model in non-dimensional equations does not account for the HF *attachment* phenomenon on the domain walls, the results demonstrated that increasing the gas flow rate significantly accelerates acid exhaustion. This response is qualitatively consistent with experimental observations reported in the literature, which consolidates the numerical approach as a promising predictive tool for gas flow optimization, leaving the development of more in-depth quantitative comparisons for future investigations.

References

[1] Abbrescia, Marcello, Vladimir Peskov, and Paulo Fonte: *Resistive Gaseous Detectors*, 2018. http://dx.doi.org/10.1002/9783527698691.

[2] Gelmi, A., O. Miguel, P. Kumari, R. Guida, and B. Mandelli: *Fluoride production in CMS Resistive Plate Chambers and aging study*. In *Proceedings of the European Physical Society Conference on High Energy Physics - EPS-HEP2019*, 2019. https://pos.sissa.it/364/108/, On behalf of the CMS Muon group and CERN-EP-DT group.

[3] Brooks, Alexander N. and Thomas J.R. Hughes: *Streamline upwind/Petrov-Galerkin formulations for convection dominated flows with particular emphasis on the incompressible Navier-Stokes equations*. Computer Methods in Applied Mechanics and Engineering, 1982.

[4] Mota, Isis Prazeres and et al: *Investigating RPC Aging: Computational Models and Insights for Enhanced Detector Longevity*. 2024. ENC-2024-0659.

[5] Mota, Isis Prazeres and et al: *RPC Aging Analysis: Computational Models and Pperspectives for Extending Detector Lifespan*. In *Proceedings of the 28th International Congress of Mechanial Engineering (COBEM 2025)*, 2025. COB-2025-2038.

[6] CMSMuonGroup: *Gas mixture quality studies for the CMS RPC detectors during LHC Run 2*. Journal of Instrumentation, 2021. https://dx.doi.org/10.1088/1748-0221/16/04/C04004.

Acknowledgment

To CAPES and FAPERJ for the financial support of this project.